

Correlated diffusion in two-dimensional systems

R. A. Tahir-Kheli and Nagwa El-Meshad

Department of Physics, Temple University, Philadelphia, Pennsylvania 19122

(Received 14 January 1985)

An equations-of-motion procedure for calculating particle diffusion in a minimally interacting, isotropic concentrated lattice gas given by Tahir-Kheli and Elliott (TKE) is known to give moderately accurate results over a wide range of concentrations in three dimensions. In two dimensions the TKE procedure and its extension to anisotropic lattices are expected to be less accurate. To test the adequacy of these theories in two dimensions, we report a variety of precision Monte Carlo simulations which have been performed in large effective samples, both isotropic and anisotropic. We find noticeable systematic differences between the predictions of the TKE theory for the intermediate-concentration regime and the Monte Carlo results. To rectify this shortcoming, we have reanalyzed the multiple rescattering of the tracer-vacancy pair, including the ensuing spatial constraints, through a sea of background particles (and vacancies) which are distributed over a two-dimensional lattice with a coordination number z . The resultant theory is found to be in very good agreement with the precision Monte Carlo data covering a wide range of particle concentrations as well as lattice anisotropies.

I. INTRODUCTION

Stochastic hopping motion of classical particles parametrized in terms of simple rate equations describes a wide range of physical phenomena. Examples include ionic motion in superionic conductors,¹ diffusion of hydrogen in various metal hydrides,² and tracer-atom diffusion in hot solids via the vacancy mechanism.³

Theoretical treatments of these phenomena in terms of unembellished, classical random-walk motions (RW) are unacceptable in that they ignore all interparticle interactions. The presence of interactions alters the details of hopping. In particular, it leads to "memory" effects that result in correlations which persist over long time intervals and macroscopic spatial separations.

In this context, it turns out that for systems in a thermodynamically disordered state, the details of the interaction (as long as it is short-ranged) are qualitatively unimportant. Accordingly, if only the zero-range hard-core repulsion is properly included in the description, the systems display the correct qualitative behavior for diffusion appropriate to interacting systems. Therefore, our attention will be focused on situations where multiple occupancy is rigorously forbidden. We shall refer to such systems as being "minimally interacting" (MI).

In MI systems, while the total-state change of the lattice gas remains governed by Markov processes, the motion of a tagged particle is not Markovian. Rather, its "random walk" is not random at all; instead, it is correlated.

Since its first observation by Bardeen and Herring,⁴ much attention has been paid to both the theory and the experiment of the phenomenon of the correlated random walk. In practice, tracer diffusion in moderately hot solids is caused by thermally produced vacancies⁵ whose concentration v is necessarily quite small (unless the system is at elevated temperatures). Thus, the original stud-

ies concentrated on the relevant limit, namely, $v = 1 - c \ll 1$.

In an important series of papers, Sankey and Fedders^{6,7} gave a diagrammatic formulation of the tracer diffusion in a MI lattice gas which forbids double occupancy but ignores all the remaining interparticle interactions. Their theory, excepting minor numerical errors, gives exact results for the tracer diffusion in the limiting concentration regimes $v \rightarrow 0$ and $v \rightarrow 1$. Moreover, it provides a reasonable interpolation in between these limits.

An entirely different procedure employing projection operator techniques was developed by Nakazato and Kitahara.⁸ Their results are applicable to a quadratic lattice in two dimensions or a simple-cubic lattice in three dimensions. Unfortunately, due to the brevity of their presentation, no discussion regarding the physical nature of their approximations is available.

Very recently, Tahir-Kheli and Elliott⁹ (TKE) presented an equations-of-motion method to calculate the entire frequency- and wave-vector-dependent response. (This response is a generalized Fourier transform of the space- and time-dependent tracer-occupancy correlation function.) In the TKE method, the essential approximation consists of decoupling the third- and the higher-body scattering contributions to the mass operator by a generalized mean-field-like procedure. The single-particle as well as some of the pair scattering corrections are taken into account and the resultant equations are reduced to quadratures. In three dimensions, for the particular case of self-diffusion, the predictions of TKE have since been tested in a detailed set of Monte Carlo simulations¹⁰ with good results.

The TKE procedure, however, suffered from an important drawback, that if the background atoms moved very slowly compared to the tracer, the rapid slowing down of the tracer in the tracer-vacancy pair was not fully iterated with respect to three- and higher-body scatterings. This

shortcoming has recently been corrected by Tahir-Kheli,¹¹ who has resummed the repeated scatterings of the tracer-vacancy pair as it travels through the lattice. The TKE theory with the Tahir-Kheli corrections (T-TKE) yields good results in three dimensions for all ratios of the tracer-background hopping rates as well as for all concentrations of the background particles.

Despite this improvement, in the intermediate concentration regime, small but noticeable systematic discrepancies were found between the T-TKE theoretical predictions and precision simulation "experiments" recently conducted by Tahir-Kheli.¹² These discrepancies are expected to become even larger as the dimensionality is reduced from three to two.

For three dimensions, Tahir-Kheli¹² also presented a detailed reanalysis of the multiple rescattering of the tracer-vacancy pair as it travels through a sea of background particles (and the vacancies). He pinpointed a subtle though significant inconsistency in the earlier T-TKE treatments,^{9,11} whereby the spatial constraints on the multiply scattered tracer-vacancy pair were not fully implemented. Indeed, in the process of such multiple scattering, the tracer-vacancy pair was originally assumed to travel unhampered as though the lattice coordination number z was effectively very large compared to unity. The new theory¹² brought fully into coincidence the precision Monte Carlo and the theoretical results in three dimensions.

Clearly, in two-dimensional quadratic or rectangular lattices the coordination number is even smaller. Accordingly, a proper accounting of the constraints dictated by the finiteness of the hopping space available to the correlated particle-vacancy pair in two dimensions is, therefore, of vital importance. To this end in Sec. II we present an appropriate reanalysis of the T-TKE^{9,11} theory for a two-dimensional isotropic square lattice which closely parallels that given for the three dimensions.¹²

In Sec. III, a description of our precision Monte Carlo simulations is given. This section concludes with an analysis of the data as well as a comparison of the simulation results with the theoretical predictions of Sec. II.

The case of the anisotropic lattice is discussed in Secs. IV and V. First the theory of Sec. II is generalized to treat the case of anisotropic hopping in two dimensions. Next, in Sec. V a detailed set of precision Monte Carlo simulation results are presented. An excellent overall agreement between the Monte Carlo results and the predictions of the theory given in Sec. IV is observed. The paper is concluded in Sec. VI with a brief comment.

II. DIFFUSION IN THE ISOTROPIC SQUARE LATTICE: THEORY

Consider a macroscopic square lattice with N sites embedded in a system where periodic boundary conditions obtain. For simplicity let us choose the units so that the nearest-neighbor separation is unity. For self-diffusion (where the hopping characteristics of the labeled particle are identical to those of the background atoms) the rate equation relevant to the MI system is the following:

$$\frac{d\sigma_i}{dt} = - \sum_j J_{ij} (\sigma_i V_j - p_j \sigma_i). \quad (2.1)$$

Here, $J_{ij} = J_{ij} = J$ if i and j are nearest neighbors. Another notation is as follows: $\sigma_i = p_i$ or n_i depending on whether the particle under study is the tracer (i.e., the labeled particle) or one of background particles. The stochastic occupancy variable σ_i has the usual significance, whereby if the site i is occupied by the appropriate particle, $\sigma_i = 1$; otherwise, $\sigma_i = 0$. A similar stochastic variable referring to a vacancy at site i is V_i . Accordingly,

$$V_i = 1 - n_i - p_i. \quad (2.2)$$

Note, that because of the MI constraints, multiple occupancy is strictly forbidden. As a result, we get

$$\sigma_i^2 = \sigma_i, \quad V_i^2 = V_i, \quad n_i V_i = 0. \quad (2.3)$$

A corollary of the above is the constraint

$$n_i p_i = p_i n_i = 0. \quad (2.4)$$

Now, following the equations-of-motion procedure described in detail by TKE in Ref. 9 and, furthermore, taking into account the multiple scattering of the particle-vacancy pair traveling in a lattice with $z \rightarrow \infty$ (as described by Tahir-Kheli in an earlier paper¹¹), we are led to an expression for the mass operator $\Sigma(\mathbf{K}, \omega)$ (see Refs. 9 and 11 for notational details) for the labeled particle propagator which has the following limiting form:

$$\lim_{\substack{K^2/\omega \rightarrow 0 \\ \omega \rightarrow 0}} \Sigma(K, \omega) = v f J k^2. \quad (2.5)$$

Here, J is the hopping rate specified in Eq. (2.1), and v and c are the vacancy and the particle concentrations, respectively,

$$\langle n_i \rangle = c, \quad \langle p_i \rangle = 1/n, \quad \langle V_i \rangle = v = 1 - c. \quad (2.6)$$

The central quantity of interest is the diffusion correlation parameter f given in Eq. (2.5). According to the procedures of Refs. 9 and 11, for a square lattice one gets

$$f^{-1} = 1 - (2c \langle \cos \theta \rangle) / [(1 + v\gamma)(1 + \langle \cos \theta \rangle)], \quad (2.7)$$

where

$$\langle \cos \theta \rangle = -0.36338023 \quad (2.8)$$

is the average cosine of the angle between successive jumps in a random walk.

The parameter γ in Eq. (2.7) is important to the understanding of the transport of the correlated particle-vacancy (composite) pair. Within the context of the TKE theory, $\gamma = 1$. Consequently, while the tracer motion is correlated overall, the motion of the tracer within the composite pair is assumed to be uncorrelated.

This shortcoming of the original TKE theory is partially overcome through the resummation procedure given in Ref. 11. As a result, the correlation of particle motion both *without* and *within* the composite pair becomes self-consistently the same. The net result of this process is that the parameter γ in Eq. (2.7) becomes equal to f .¹¹

Despite the major qualitative improvement in the

theory, especially with regard to diffusion through a relatively slow background,¹¹ the resummation of the repeated scattering of the correlated tracer-vacancy pair is not fully accurate in finite lattices. The basic reason for this remaining deficiency lies in the fact that the available hopping space for the correlated pair is restricted in view of the finite coordination number of the lattice.

Tahir-Kheli very recently considered this aspect of the problem in three dimensions¹² and calculated the effects arising out of the finiteness of the available hopping space to the correlated nearest-neighbor particle-vacancy pair. This adjustment,¹² it turns out, can readily be incorporated into the previous theory [see Eq. (2.7)]. The net result is a renormalized γ , i.e.,

$$\gamma = f(c)\mu. \quad (2.9)$$

In the above, the parameter μ embodies the constraints imposed by the finiteness of the coordination number z as well as the finiteness of the particle concentration c (or, equivalently, that of the vacancy concentration v). Because of the symmetry between the particle-vacancy pair, Tahir-Kheli¹² finally gets

$$\begin{aligned} \mu(z, c, v) &= \mu(z, v, c) = \mu \\ &= 1 + 4 \sum_{i=1}^z [(cv)^i (2z - 1 - i)! / (2z - 1)!]. \end{aligned} \quad (2.10)$$

For isotropic systems, the lattice dependence of the above result enters only through the coordinate number z . Substituting $z=4$ for a square lattice, the resultant Eqs. (2.7)–(2.10) comprise a simple transcendental relationship that is readily solved numerically.

III. DIFFUSION IN THE ISOTROPIC SQUARE LATTICE

A. Simulation

Numerical Monte Carlo simulations of labeled particle diffusion in three dimensions have been performed by many different workers.^{13,14} Two-dimensional simulations, though easier to perform, have seemingly been less popular.^{15,16} (However, several years ago Kutner¹⁷ studied tracer diffusion in an isotropic square lattice. In his work, Kutner analyzed a system with 50×50 sites with periodic boundary conditions. However, his data are rather preliminary in character and show considerable degree of scatter.)

The objective of the present exercise is to compute precision results for the tracer diffusion in both the isotropic square and the anisotropic rectangular lattices. Let us describe first the isotropic square lattice.

B. Procedure

Construct a finite, $N \times N$ grid and impose periodic boundary conditions on it. Next, randomly distribute a predetermined concentration c of atoms on the grid. Then, execute the following steps seriatim:

(0) Label all particles $1, 2, 3, \dots, N'$, where $N' = cN$.

(1) Randomly select one of these N' particles as a candidate for hopping.

(2) Select, with the roll of an appropriate four-sided

dice (i.e., a random-number generator), a nearest-neighbor site of the chosen particle to determine the direction in which the particle is to attempt its move.

(3) Check if the neighboring site in the intended direction of the hop is in fact empty. If the relevant site is occupied, abandon the attempt and return to step (1) above. On the other hand, if the site to be hopped onto is empty, execute the hop and relabel the coordinates of that atom to reflect its new location.

(4) Return to step (1) above and randomly choose once again one of the N' particles as a candidate for hopping.

(5) When the step (1) has been performed a total of N' , a single unit of Monte Carlo time has elapsed—otherwise to be denoted as a Monte Carlo step per particle (MCS/ p).

The foregoing procedure is carried out for a large number of MCS/ p units. (We shall call this number τ .) Note that a convenient method for comparing the theoretical predictions and the numerical simulation results obtained here is to transform the tracer hopping rate J to the MCS/ p units, i.e., to write $J = \frac{1}{4}$. For self-diffusion, this simulation procedure yields good statistics because each one of the particles can be independently treated as the distinct tracer.

A complete record of the history of all the particles in the system is kept, including a shadow of their positions on a lattice extending indefinitely in all four directions. At the conclusion of the simulation, this information is translated into mean-square displacement of an average tracer as a function of the elapsed Monte Carlo time. In the limit of long time, the Einstein relation leads naturally to the diffusion coefficient of the tracer, which in turn specifies the correlation factor $f(c)$.

For particle concentrations $c > 0.5$, lattice networks of sizes 100×100 and 150×150 were used. For smaller concentrations, the networks used were somewhat larger, i.e., 150×150 and 200×200 . The objective in working with two different sizes was to search for any possible sensitivity of the results to the network sizes, or equivalently, to look for the so-called boundary effects.

In order to achieve good statistics, necessary for a precision determination of the diffusion coefficient [or equivalently, the correlation factor $f(c)$], an ensemble of such subsamples was utilized, thus making the total number of labeled particles (whose histories are traced from $\tau=0$ to $\tau \sim 10^3 - 10^4$ MCS/ p) over a million for each measurement. Results for the individual subsamples were thus combined to form an effective grand sample (GS) consisting of $N_G \sim 10^6$ or more particles. The averages over such GS's are subject to natural fluctuations of the order $\sim (N_G)^{-1/2}$, which in practice worked out to a few parts per thousand.

In addition to the precision results obtained from GS's for which $N_G > 10^6$, we have also worked with mini-GS's (MGS), each totaling approximately 40 000–60 000 particles. Averages over such smaller samples (namely, the MGS's) were of course subject to 3–5 times larger errors, which generally amounted to somewhere between one-half a percent to two and one-half percent overall. However, because of the relative ease with which these less accurate results could be obtained (the total computational effort is linearly proportional to the effective size N_G of the sys-

tem being studied), they were deemed useful in forming a qualitative picture of the diffusion characteristics of the physical system.

C. Analysis

Before describing the various results, it is appropriate that the procedure for analyzing the data be specified. In a "perfect" simulation of the isotropic hopping case, the results for the mean-square displacement along the x and the y directions, i.e., $\langle \Delta^2 x \rangle_{(\tau)}$ and $\langle \Delta^2 y \rangle_{(\tau)}$, should be identical. In practice, of course, this is not exactly true. Thus, the equality of $\langle \Delta^2 x \rangle_{(\tau)}$ and $\langle \Delta^2 y \rangle_{(\tau)}$ provides a good check on the accuracy of the data. Also, it affords additional insight into the fluctuations inherent in the simulation that has been conducted.

The mutual differences between the computed results for $\langle \Delta^2 x \rangle_{(\tau)}$ and $\langle \Delta^2 y \rangle_{(\tau)}$ were found to be of the same order as our expectations of the natural fluctuations of the relevant data—namely, they were of the order of one to five parts per thousand for GS's consisting of $\sim 10^6$ particles each. In view of this, for the isotropic case we combined $\langle \Delta^2 x \rangle_{(\tau)}$ with $\langle \Delta^2 y \rangle_{(\tau)}$ and took their average to obtain the "best" available data for the mean-square displacement Δ^2 . This data consisted of Δ^2 versus the MCS/ p time τ , for τ ranging between 0 and 2500. In two dimensions, for general concentrations the occurrence of a weak logarithmic term is indicated in the expansion of the TKE mass operator (2.5). In the time domain it leads to the following expansion for the mean-square displacement at long times:

$$\Delta^2(\tau) = S_0\tau + S_1 + S_2 \ln(\tau) + O(1/\tau J), \quad J\tau \gg 1 \quad (3.1)$$

where S_0 , S_1 , and S_2 are constants. The tracer diffusion coefficient, or more conveniently the diffusion correlation factor $f(c)$, is directly related to the slope S_0 , i.e.,

$$f(c) = S_0 / [2J(1-c)]. \quad (3.2)$$

For an accurate determination of the correlation factor $f(c)$, it was found best to proceed as follows: choose a starting time τ_0 (which should be long compared to unity). In practice, for the two-dimensional, isotropic case the long-time behavior was found to have set in when τ_0 was approximately 100. (This applied to $c = \frac{1}{2}$. For smaller concentrations, the appropriate τ_0 is proportionately longer.)

For any such long-time-limit choice of τ_0 , we first determine the quantities $\alpha(\tau_i - \tau_0)$,

$$\alpha(\tau_i - \tau_0) = \Delta^2(\tau_i) - \Delta^2(\tau_0), \quad (3.3)$$

where τ_i is larger than τ_0 . Using Eq. (3.1), the constant S_1 is eliminated by the use of the following process:

$$\alpha(\tau_i - \tau_0) = S_0(\tau_i - \tau_0) + S_2 \ln(\tau_i/\tau_0). \quad (3.4)$$

Next, upon carrying out the same operation for another suitable time τ_j , larger than both τ_i and τ_0 , we get

$$\alpha(\tau_j - \tau_0) = S_0(\tau_j - \tau_0) + S_2 \ln(\tau_j/\tau_0). \quad (3.5)$$

Using Eqs. (3.4) and (3.5) the second unknown constant S_2 is eliminated. This gives

$$\begin{aligned} & [\alpha(\tau_j - \tau_0)] / \ln(\tau_j/\tau_0) - [\alpha(\tau_i - \tau_0)] / \ln(\tau_i/\tau_0) \\ & = S_0 [(\tau_j - \tau_0) / \ln(\tau_j/\tau_0) - (\tau_i - \tau_0) / \ln(\tau_i/\tau_0)]. \end{aligned} \quad (3.6)$$

The slope S_0 is thus easily evaluated from Eq. (3.6). Elementary division leads to the following:

$$\begin{aligned} S_0 &= Q/U, \\ Q &= [\alpha(\tau_j - \tau_0)] / \ln(\tau_j/\tau_0) \\ &\quad - [\alpha(\tau_i - \tau_0)] / \ln(\tau_i/\tau_0), \\ U &= (\tau_j - \tau_0) / \ln(\tau_j/\tau_0) - (\tau_i - \tau_0) / \ln(\tau_i/\tau_0). \end{aligned} \quad (3.7)$$

If the data were perfect (namely, if there were absolutely no fluctuations in the data), and if the starting time τ_0 was infinitely long, the slope S_0 would be independent of τ_0 . In practice, however, neither are the data perfect nor is τ_0 really long. As a consequence, the single parameter S_0 , determined from Eq. (3.7), is a function of τ_0 as well as the times τ_i and τ_j . In order to refine this procedure and reduce possible errors in the analysis to a minimum, the following cyclic procedure was followed.

Because the data for Δ^2 as a function of time τ are known for say a hundred different equally spaced values of τ ranging between 25 and 2500, for any given initial time $\tau_0 \geq 100$, we find the slope $S(\tau_0, \tau_i, \tau_j)$ for all the different allowed values of τ_i and τ_j , where $\tau_j > \tau_i > \tau_0$, with the maximum values of τ_j fixed at a point conveniently below 2500. In practice, we choose this maximum value for $\tau_j = 2000 = \tau_m$. This procedure helps reduce the "end fluctuations" which can arise due to the shortness of the final span.

Thus, for a given τ_0 a large number of estimates for $S(\tau_0, \tau_i, \tau_j)$ are assembled. These estimates are then averaged to obtain the best value for $S(\tau_0)$. (Note, for $\tau_m > \tau_j > \tau_i > \tau_0 > 100$ and $\tau_m = 2000$ for the present case, the ensemble to be averaged over can be quite large.) Moreover, a root-mean-square deviation $\delta(\tau_0)$ from such an average $S(\tau_0)$ of the various results for $S(\tau_0, \tau_i, \tau_j)$ is also obtained. This number, $\delta(\tau_0)$, thus provides a useful measure of the fluctuations inherent in the evaluation of $S(\tau_0)$. Having determined $S(\tau_0)$ and a measure of its error $\delta(\tau_0)$, the process is repeated by raising the starting value of the time τ_0 by 50 units until $\tau_0 = 1800$ is reached.

It is clear that there are two competing processes in operation here. One of these causes the effective accuracy of the processed data to be higher the smaller the starting value τ_0 . This is because the average is taken over a larger ensemble of values for $S(\tau_0, \tau_i, \tau_j)$. On the other hand, it is also true that as τ_0 becomes larger, the terms that are ignored in Eq. (3.1), i.e., terms proportional to $1/\tau_0$, become progressively less important. Consequently, the implicit accuracy of the above-mentioned routine increases for larger τ_0 . Fortunately, these processes are somewhat complementary in their effects—one becomes more accurate as τ_0 rises while the other decreases in accuracy.

It is of course very difficult to put precise quantitative values on these two effects. Nevertheless, a reasonable compromise is to take a grand average of the $S(\tau_0)$'s so obtained over the entire spectrum of τ_0 's extending from

$\tau_0=100$ to $\tau_0=1800$. This average, to be called S , is then assumed to be subject to an error of order δ , which is taken to be the square root of the average of $\delta^2(\tau_0)$'s taken over all the different starting times τ_0 's so used.

The finite-size, or equivalently, the boundary effects are another possible source of error. A systematic analysis of these effects is time consuming to undertake. Nevertheless, from previous work on diffusion in two-^{15,16} and three-^{10,13,14} dimensional systems, it is clear that, at least for the isotropic cases, the finite-size effects are small as long as the root-mean-square displacements along any of the Cartesian axes are "small" compared to the relevant linear dimensions of the lattice used. For the present simulations, such a condition is seemingly well satisfied. In the same vein, the use of two different size networks, both quite large but yet differing by an approximate factor of 2 in overall size, provides a reasonable qualitative feel for the size dependence. To this end, for $c \sim 0.6$ and 0.4, complete simulations of effective GS sizes of $\sim 10^6/2$ particles were carried out with both sizes of networks, i.e., $N=100$ and 150 and $N=150$ and 200, respectively. The mutual differences between the data were very similar to the root-mean-square fluctuations in each. Accordingly, these results were combined to form the final best data.

D. Results

For ready comparison, in Table I the theoretical results are listed alongside those obtained from our large grand-sample precision simulations. The predictions of the TKE theory are seen to be a little too high over the entire range of concentrations. In particular, the TKE theory performs worst in the intermediate region, i.e., $0.8 < c < 0.4$, where it differs from the Monte Carlo results

TABLE I. The diffusion correlation factor $f(c)$ for isotropic nearest-neighbor hopping on a square lattice is given as a function of the background concentration c . The table refers to the precision simulation case where the effective sizes N_G of the grand samples were at least 10^6 particles. The concentration c is listed in the first column and the best simulation results for the factor $f(c)$, along with the relevant root-mean-square deviation, are listed in the second column. The third and the fourth columns list the corresponding theoretical results for $f(c)$ as provided by the present improved theory and the earlier TKE theory, respectively.

| Background particle concentration c | Precision simulation results | $f(c)$ | |
|---------------------------------------|------------------------------|----------------|--------------------|
| | | Present theory | Earlier TKE theory |
| 0.9002 | 0.507±0.003 | 0.5062 | 0.5171 |
| 0.8002 | 0.552±0.003 | 0.5509 | 0.5679 |
| 0.6991 | 0.604±0.003 | 0.6008 | 0.6193 |
| 0.6000 | 0.657±0.003 | 0.6548 | 0.6715 |
| 0.5001 | 0.710±0.003 | 0.7117 | 0.7244 |
| 0.4002 | 0.767±0.003 | 0.7699 | 0.7779 |
| 0.3003 | 0.824±0.004 | 0.8281 | 0.8323 |
| 0.2002 | 0.882±0.004 | 0.8859 | 0.8874 |

TABLE II. Similar to Table I except that here we give the less accurate simulation results, for the same system, obtained from GS with approximately 50 000 particles each. Roughly speaking, these results are subject to errors three to five times larger.

| Background particle concentration c | $f(c)$ | | |
|---------------------------------------|---------------------------------|----------------|--------------------|
| | Small-sample simulation results | Present theory | Earlier TKE theory |
| 0.9550 | 0.48±0.010 | 0.4839 | 0.4894 |
| 0.8550 | 0.52±0.010 | 0.5257 | 0.5398 |
| 0.7550 | 0.57±0.010 | 0.5728 | 0.5909 |
| 0.6550 | 0.63±0.015 | 0.6247 | 0.6427 |
| 0.5550 | 0.68±0.015 | 0.6801 | 0.6952 |
| 0.4550 | 0.73±0.015 | 0.7378 | 0.7484 |
| 0.3550 | 0.79±0.015 | 0.7962 | 0.8023 |
| 0.2550 | 0.85±0.015 | 0.8544 | 0.8570 |

by approximately 2%. The present theory, on the other hand, lies within 0.5 to 3 parts per thousand of the simulation results. Of course, not much attention should be paid to this discrepancy because it is similar to the inherent error of these "precision" simulations.

In order to get an additional qualitative picture of these results, in Table II we report a set of results obtained from mini grand samples with sizes varying between 40 000 to 60 000 particles each. Also, to aid the eye, the results for the diffusion correlation factor f given in Tables I and II are plotted in Fig. 1. The solid dark circles represent the precision results of Table I, whereas the crosses indicate the generally less accurate results of Table II. (Note that the size of the circles and crosses is *not* representative of the error δ . This error is specified instead in the tables.)

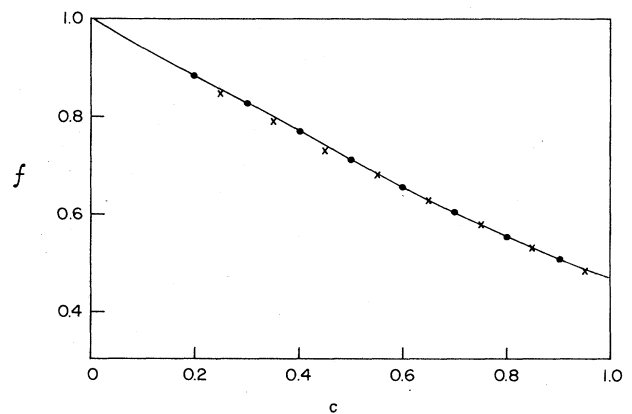


FIG. 1. Correlation factor $f(c)$ is given as a function of the concentration c for the tracer diffusion in a simple square isotropic lattice. The solid curve represents our theoretical results, the solid circles show the large GS precision simulation results, and the crosses represent the less accurate small-sample simulation results described in Table II. (Note the size of the circles or crosses bears no relationship to the accuracy of the points.)

IV. ANISOTROPIC DIFFUSION: THEORY

Let us consider next an anisotropic, two-dimensional rectangular lattice. For anisotropic lattices, Tahir-Kheli¹⁸ gave a treatment based on the original TKE theory for isotropic lattices. Without going into details of the rather cumbersome algebra, it is convenient to mention one or two salient aspects of the results. The new feature added is that the correlation factor has directional dependence as well as dependence on the ratios of the hopping integrals along the various directions. For a hypercubic lattice of dimensionality d , these results are contained in Eqs. (3.9)–(3.10c) of Ref. 18.

Because the essential procedure of Ref. 18 is an outgrowth of that used in the TKE theory, it too suffers from an incomplete summation of the particle-vacancy composite pair scattering contribution. A partial correction of this shortcoming, paralleling that described earlier for the isotropic case, has been given by Tahir-Kheli.¹⁹ While the reader is again best referred to the source for details,¹⁹ it is convenient to record the final form of the results. The tracer correlation factor f for diffusion along a Cartesian direction β is specified by the following set of self-consistent relationships:

$$\begin{aligned} f_\beta &= 1 + 2cT_\beta/[1 - (2c - 1 - vf_\beta)T_\beta], \\ T_\beta &= (1/N) \sum_\lambda J_\beta [\cos(2\lambda_\beta a_\beta) - 1]/Y(\lambda), \\ Y(\lambda) &= 2 \sum_\alpha J_\alpha (1 + vf_\alpha) [1 - \cos(\lambda_\alpha a_\alpha)]. \end{aligned} \quad (4.1)$$

Here, $\beta, \alpha = x, y, z, \dots, d$; J_β is the particle hopping rate along direction β , where the nearest-neighbor separation is a_β . For isotropic hopping, the above reduces to the simple form contained in Eq. (2.7) with $\gamma = f$.

Despite the partial resummation of the composite pair scattering, much like the isotropic case, the foregoing ignores all the spatial constraints imposed on the transport of the nearest-neighbor composite pair. Again, Tahir-Kheli¹² has supplied the more complete resummation which includes the spatial constraints for a three-dimensional anisotropic lattice. It is a simple matter to extend his analysis to a two-dimensional rectangular lattice with nearest-neighbor separations a_x and a_y . We get

$$\begin{aligned} f_x &= 1 + 2c\Gamma_x/[1 - (2c - 1 - vf_x\mu_x)\Gamma_x], \\ \Gamma_x &= (1/2N) \sum_\lambda J_x [\cos(2\lambda_x a_x) - 1]/E(\lambda), \\ E(\lambda) &= J_x (1 + vf_x\mu_x) [1 - \cos(\lambda_x a_x)] \\ &\quad + J_y (1 + vf_y\mu_y) [1 - \cos(\lambda_y a_y)]. \end{aligned} \quad (4.2)$$

The correlation factor for diffusion along the y direction is given analogously to (4.2). (To this end, one merely interchanges the indices $x \leftrightarrow y$.)

The parameters μ_x and μ_y embody the spatial constraints for diffusion along the x and the y directions:

$$\mu_x = 1 + 4 \sum_i^{z_x} (cv)^i (2z_x - 1 - i)! / (2z_x - 1)!, \quad (4.3)$$

where

$$z_x = z(J_x + J_y)/(2J_x). \quad (4.4)$$

The sum on the right-hand side of Eq. (4.3) is to be carried through to the largest integral value associated with the number z_x . (Again, in the above the parameters μ_y may be obtained simply through the interchange $x \leftrightarrow y$.) For $\eta = 1$, $\mu_x = \mu_y = \mu$, given previously in Eq. (2.10) for the isotropic case.

It is to be noted that the effective hopping space along the slow direction enlarges. Similarly, the space shrinks along the fast direction. For instance, in the limit when $J_x \rightarrow 0$, the hopping along the y direction becomes one dimensional and thus $z_y \rightarrow 2$. The solution of the self-consistent relations for f_x and f_y , given in Eqs. (4.2) and (4.3), can be obtained by simple numerical procedures.

V. DIFFUSION IN THE ANISOTROPIC LATTICE

A. Simulation

In anisotropic, two-dimensional rectangular lattices of the form described in the preceding section, simulations have to deal with the essential fact that the hopping rates along the two directions are unequal. However, because the grid is denumerated numerically, the difference between the nearest-neighbor separations along the mutually orthogonal x and y directions is not a relevant variable. It can enter into discussion only if the wave-vector-dependent properties of the system are examined, and even then, it is only the dimensionless variable ($k_\alpha a_\alpha$) along the directions $\alpha = x, y$, rather than k_α by itself, which is the relevant quantity.

Because the computer program representing the rate equations that specify the hopping probabilities determines the numerical value of the sum of hopping rates J_x and J_y along the two directions, i.e.,

$$J_x + J_y = \frac{1}{2}, \quad (5.1)$$

we are left with a single independent parameter η in the problem, i.e.,

$$\eta = J_x/J_y. \quad (5.2)$$

The background hopping rates are once again taken to be identical to that of the tracer, and accordingly any of the N'_G atoms that comprise a given subsample can independently be considered as tracers.

Because J_x is not equal to J_y , the mean-square displacements along the two directions are also different. In any simulation, therefore, both $\langle \Delta x^2 \rangle_{(t)}$ and $\langle \Delta y^2 \rangle_{(t)}$ have to be recorded. Indicated below are two possible simulation routines.

Given the concentration c and the ratio η , randomly occupy a lattice of size N with $N' = cN$ atoms. Set

$$R = \eta/(1 + \eta). \quad (5.3)$$

After randomly choosing one of the N' atoms as a candidate for hopping, call a random number r where $0 < r < 1$. According to the first procedure (I), the direction of the attempted hop of the chosen particle is determined entirely by the value of r via the following prescription:

(a) For $0 < r < R/2$, the attempted move is in the $+x$ direction.

(b) For $R/2 < r < R$, it is in the $-x$ direction.

(c) For $R < r < (1+R)/2$, the move is along the $+y$ direction.

(d) Finally, if $(1+R)/2 < r < 1$, the move is along the $-y$ direction.

The second procedure (II) is somewhat simpler but involves two calls r_1 and r_2 to the random-number generator. If $r_1 < R$, the atom attempts to hop along the $\pm x$ directions; otherwise, the attempted hop is along the $\pm y$ axis. The choice between the $+$ or $-$ directions is made next, according to whether r_2 is less or more than 0.5.

Depending on the concentration and the size of the lattice, procedure I gives an overall saving of between 5% to 15% of the total computing time. On the other hand, the results of the second procedure are generally somewhat smoother. This was particularly so for small ratios of η where we exclusively used procedure II. (For $\eta \sim 0.3-1$, both the procedures gave equally good results.) These simulations were generally run for 5000 MCS/ p each.

B. Analysis

Although the mean-square displacements along the x and y directions are in general different, once an appropriately large sample consisting of an effective total number of hopping tracers equal to $N_G \geq 10^6$ has been simulated, the analysis follows a pattern similar to that used for the isotropic case discussed above. That is, the mean-square displacement for time τ along the axis $\beta=x, y$, i.e., $\Delta_\beta^2(\tau)$ is represented as follows:

$$\Delta_\beta^2(\tau) = S_0^\beta \tau + S_1^\beta + S_2^\beta \ln(\tau) + O(1/(J_\beta \tau)), \quad J_\beta \tau \gg 1. \quad (5.4)$$

The procedure for obtaining the best fit to the relevant coefficient S_0^β , as well as for estimating the size of the possible error in this evaluation, is identical to that described in detail for the isotropic case. The only difference that arises here is that now there are two correlation factors $f_\beta(c)$, $\beta=x, y$, and accordingly we have two equations of the type

$$f_\beta(c) = D^\beta / D_0^\beta = S_0^\beta / [2J_\beta(1-c)]. \quad (5.5)$$

[The numerical value of the hopping rates in units of the inverse Monte Carlo time is readily specified through the simple relationships (5.1) and (5.2).]

The next important issue to be dealt with is the nature of the long-time limit. In other words, while for the isotropic case it was straightforward to determine the appropriate long-time limit as being the one for which we obtain $J\tau \gg 1$, where $J = \frac{1}{4}$, the corresponding statements in the case of anisotropic hopping are less trivial to make.

It is, nevertheless, clear that as long as η is not much less than unity, i.e., for

$$1 > \eta > \frac{1}{5}, \quad (5.6)$$

the times τ which are ≥ 600 or so do satisfy the requirement of being reasonably long. This is readily confirmed as follows: When Eq. (5.6) holds, we get

$$\begin{aligned} J_x \tau &= \eta \tau / [2(1+\eta)] \geq 50, \\ J_y \tau &= \tau / [2(1+\eta)] \geq 250. \end{aligned} \quad (5.7)$$

On the other hand, for highly anisotropic systems for which η is much less than unity, the hopping along the fast direction is essentially one dimensional. That is, the physical system now consists of only "weakly coupled" linear chains which run parallel to the y axis. Accordingly, it is important to be aware of the pseudo-one-dimensionality of such a system that obtains in the limit $\eta \ll 1$. Equally, it is essential to bear in mind that a naive argument, which worked in Eq. (5.7), is altogether unsatisfactory for the case $\eta \ll 1$. Here, the logic that led to Eq. (5.7) would give

$$\begin{aligned} J_y \tau &= \tau / [2(1+\eta)] \sim \tau/2, \\ J_x \tau &\sim \eta \tau / [2(1+\eta)] \sim \tau \eta / 2. \end{aligned} \quad (5.8)$$

That is, it would appear that we need very long times of order $100\eta^{-1}$ or so to achieve the so-called "long-time-limit behavior" along the slow x direction. On the other hand, the long-time along the fast y direction is expected to be achieved relatively early, i.e., for times $\tau \sim 100$ MCS/ p or thereabouts.

The fact of the matter is entirely different. Along the fast y direction, the pseudo-one-dimensionality gives rise to a characteristic $t^{1/2}$ dependence which lasts throughout the intermediate time regime. For instance, in the case $c = \frac{1}{2}$ and $\eta \sim 10^{-3}$, the intermediate state lasts approximately from 250 to 1000 MCS/ p . The Einstein limit, which is characteristic of the two- or higher-dimensional systems, sets in much later. That is, for $c = \frac{1}{2}$, this limit obtains around 1500 MCS/ p when $\eta \sim 10^{-3}$. Thus, along the fast y direction, we need to run the simulations for at least 4000–5000 MCS/ p if we want to get satisfactory statistics for the $c = \frac{1}{2}$ system with η of the order of 10^{-3} . On the other hand, for $\eta \sim 10^{-2}$, we can get away with times of order 3000 MCS/ p .

In contrast to the first direction, the diffusive classical behavior sets in very rapidly along the slow x direction. Here, the tracer motion is essentially of the mean-field, random-walk type beginning at fairly "early times," i.e., when $J_x \tau \sim 1$. The reason for this interesting reversal of roles lies in the rapid equilibration of the background (which occurs because of the y -directed hops). By the time the tracer has taken a single hop along the x direction, on the average the background has had time to execute approximately η^{-1} hops. Thus, the tracer, while moving in the x direction, appears to be surrounded by a simple mean-field background. Accordingly, for $\eta \rightarrow 0$, $f_x(x)$ approaches the uncorrelated limit of unity¹⁸ and, moreover, in the slow direction the "long-time" behavior sets in as early as the corresponding intermediate-time $t^{1/2}$ behavior in the y direction. Because both the mean-square displacements (i.e., along the x and y directions) are measured in the course of a single simulation, in practice we need concern ourselves with achieving long-time equilibration only in the fast direction.

C. Results

In Table III we have listed the various sets of results for the tracer diffusion correlation factors $f_\beta(c)$, $\beta=x, y$ in anisotropic two-dimensional rectangular lattices. Here, in

TABLE III. The diffusion correlation factors $f_x(c)$ and $f_y(c)$ are listed for an anisotropic two-dimensional rectangular lattice for different values of the background particle concentration. The anisotropy in the hopping rates is specified by their ratio $\eta=J_x/J_y$. The overall effective size of the samples is $\geq 10^6$ particles.

| η | Background particle concentration c | Theoretical results | | | | | |
|------------------|---------------------------------------|------------------------------|-------------|----------------|--------|--------------------------------------|--------|
| | | Precision simulation results | | Present theory | | Earlier TKE-like theory ^a | |
| | | f_x | f_y | f_x | f_y | f_x | f_y |
| 1 | 0.800 20 | 0.552±0.003 | 0.552±0.003 | 0.5509 | 0.5509 | 0.5677 | 0.5677 |
| $\frac{1}{3}$ | 0.799 46 | 0.702±0.004 | 0.395±0.004 | 0.6992 | 0.3919 | 0.7147 | 0.4080 |
| $\frac{1}{9}$ | 0.800 14 | 0.813±0.004 | 0.257±0.004 | 0.8113 | 0.2549 | 0.8235 | 0.2685 |
| $\frac{1}{24}$ | 0.800 25 | 0.880±0.004 | 0.169±0.004 | 0.8798 | 0.1654 | 0.8886 | 0.1761 |
| $\frac{1}{99}$ | 0.800 13 | 0.944±0.006 | 0.085±0.002 | 0.9391 | 0.0848 | 0.9440 | 0.0914 |
| $\frac{1}{499}$ | 0.799 74 | 0.966±0.010 | 0.040±0.002 | 0.9729 | 0.0390 | 0.9754 | 0.0424 |
| $\frac{1}{1999}$ | 0.799 95 | 0.986±0.010 | 0.020±0.002 | 0.9884 | 0.0185 | 0.9897 | 0.0197 |
| 1 | 0.499 92 | 0.710±0.003 | 0.710±0.003 | 0.7117 | 0.7117 | 0.7244 | 0.7244 |
| $\frac{1}{3}$ | 0.500 39 | 0.827±0.005 | 0.561±0.003 | 0.8223 | 0.5624 | 0.8333 | 0.5790 |
| $\frac{1}{9}$ | 0.500 27 | 0.893±0.005 | 0.398±0.003 | 0.8934 | 0.4013 | 0.9032 | 0.4232 |
| $\frac{1}{24}$ | 0.500 75 | 0.937±0.005 | 0.277±0.004 | 0.9329 | 0.2752 | 0.9409 | 0.2991 |
| $\frac{1}{99}$ | 0.499 73 | 0.964±0.005 | 0.150±0.004 | 0.9662 | 0.1474 | 0.9712 | 0.1676 |
| $\frac{1}{499}$ | 0.499 19 | 0.984±0.008 | 0.071±0.003 | 0.9849 | 0.0690 | 0.9876 | 0.0815 |
| $\frac{1}{1999}$ | 0.499 45 | 0.992±0.008 | 0.036±0.003 | 0.9933 | 0.0337 | 0.9949 | 0.0387 |

^aReference 18.

TABLE IV. Diffusion correlation factors for anisotropic hopping, with $\eta=0.1$, in a two-dimensional rectangular lattice, are given as a function of the background concentration c . Here the effective sample sizes were $\sim 50\,000$ particles.

| Background concentration c | Theoretical results | | | | | |
|------------------------------|---------------------------------|-------------|----------------|--------|--------------------------------------|--------|
| | Small-sample simulation results | | Present theory | | Earlier TKE-type theory ^a | |
| | f_x | f_y | f_x | f_y | f_x | f_y |
| 0.9500 | 0.786±0.005 | 0.199±0.004 | 0.7804 | 0.1996 | 0.7848 | 0.2032 |
| 0.9000 | 0.799±0.005 | 0.214±0.004 | 0.7935 | 0.2129 | 0.8013 | 0.2200 |
| 0.8500 | 0.801±0.005 | 0.231±0.005 | 0.8068 | 0.2276 | 0.8169 | 0.2379 |
| 0.8000 | 0.815±0.006 | 0.246±0.005 | 0.8201 | 0.2438 | 0.8319 | 0.2571 |
| 0.7500 | 0.825±0.006 | 0.266±0.005 | 0.8334 | 0.2618 | 0.8461 | 0.2778 |
| 0.7000 | 0.842±0.006 | 0.276±0.005 | 0.8468 | 0.2818 | 0.8597 | 0.3000 |
| 0.6500 | 0.851±0.007 | 0.305±0.005 | 0.8600 | 0.3039 | 0.8726 | 0.3240 |
| 0.6000 | 0.880±0.007 | 0.334±0.005 | 0.8731 | 0.3286 | 0.8850 | 0.3500 |
| 0.5500 | 0.890±0.007 | 0.354±0.006 | 0.8860 | 0.3562 | 0.8969 | 0.3783 |
| 0.5000 | 0.905±0.070 | 0.393±0.060 | 0.8986 | 0.3869 | 0.9082 | 0.4091 |
| 0.4500 | 0.905±0.080 | 0.431±0.006 | 0.9109 | 0.4211 | 0.9191 | 0.4429 |
| 0.4000 | 0.932±0.008 | 0.465±0.060 | 0.9228 | 0.4594 | 0.9296 | 0.4800 |
| 0.3500 | 0.925±0.009 | 0.495±0.006 | 0.9343 | 0.5023 | 0.9396 | 0.5210 |
| 0.3000 | 0.950±0.019 | 0.542±0.006 | 0.9452 | 0.5503 | 0.9492 | 0.5667 |
| 0.2500 | 0.943±0.010 | 0.592±0.009 | 0.9557 | 0.6042 | 0.9585 | 0.6176 |
| 0.2250 | 0.954±0.015 | 0.635±0.010 | 0.9607 | 0.6336 | 0.9630 | 0.6455 |
| 0.2000 | 0.974±0.015 | 0.665±0.010 | 0.9656 | 0.6648 | 0.9674 | 0.6750 |
| 0.1500 | 0.980±0.015 | 0.725±0.012 | 0.9750 | 0.7332 | 0.9760 | 0.7400 |
| 0.1000 | 0.981±0.015 | 0.800±0.015 | 0.9838 | 0.8107 | 0.9843 | 0.8143 |

^aReference 18.

TABLE V. The diffusion correlation factors for anisotropic hopping for the background concentration $c=0.5000$, in a two-dimensional rectangular lattice, are given for different values of the ratio η . The effective sample sizes were $\sim 50\,000$ particles.

| η | Small-sample simulation results | | Theoretical results | | | |
|-----------------|---------------------------------|-------------|---------------------|--------|--------------------------------------|--------|
| | f_x | f_y | Present theory | | Earlier TKE-like theory ^a | |
| | f_x | f_y | f_x | f_y | f_x | f_y |
| $\frac{2}{3}$ | 0.762±0.015 | 0.656±0.005 | 0.7576 | 0.6602 | 0.7695 | 0.6740 |
| $\frac{3}{7}$ | 0.801±0.015 | 0.579±0.005 | 0.8009 | 0.5991 | 0.8122 | 0.6146 |
| $\frac{1}{5}$ | 0.864±0.015 | 0.489±0.008 | 0.8597 | 0.4871 | 0.8703 | 0.5061 |
| $\frac{7}{93}$ | 0.915±0.015 | 0.354±0.008 | 0.9114 | 0.3484 | 0.9205 | 0.3715 |
| $\frac{5}{95}$ | 0.927±0.015 | 0.304±0.008 | 0.9252 | 0.3030 | 0.9336 | 0.3269 |
| $\frac{1}{24}$ | 0.930±0.015 | 0.278±0.008 | 0.9331 | 0.2756 | 0.9410 | 0.2995 |
| $\frac{3}{97}$ | 0.940±0.015 | 0.248±0.008 | 0.9420 | 0.2431 | 0.9493 | 0.2669 |
| $\frac{1}{49}$ | 0.945±0.020 | 0.202±0.008 | 0.9525 | 0.2028 | 0.9589 | 0.2257 |
| $\frac{1}{249}$ | 0.983±0.020 | 0.096±0.008 | 0.9784 | 0.0956 | 0.9820 | 0.1116 |
| $\frac{1}{999}$ | 0.991±0.020 | 0.043±0.008 | 0.9896 | 0.0490 | 0.9917 | 0.0577 |

^aReference 18.

addition to the results obtained from present theory, are also listed those predicted by the earlier TKE-like theory given by Tahir-Kheli.¹⁸

The simulations listed in Table III are the extensive, large-sample studies involving $N_G \geq 10^6$ tracers. For reasonable values of the anisotropy, that is, where η is no smaller than, say, $\frac{1}{10}$, these results are expected to yield precision estimates for $f_\beta(c)$ such that the expected error is not more than two or three parts per thousand. However, for very small η 's (i.e., for systems with very large anisotropies), practical limitations on the available computer time as well as the available memory size on the CDC-

Cyber 170-750 system have forced us into accepting proportionately larger errors (see Table III).

As for the isotropic lattice, for the anisotropic system we have also performed small GS simulations involving 40 000–60 000 particles each. These results are necessarily less precise but because of the relative ease with which they are obtained, they are useful for yielding an overall, qualitative picture of the problem. Such results are given in Tables IV (which refers to $\eta=0.1$) and V (referring to $c=0.5000$) and Figs. 2 and 3.

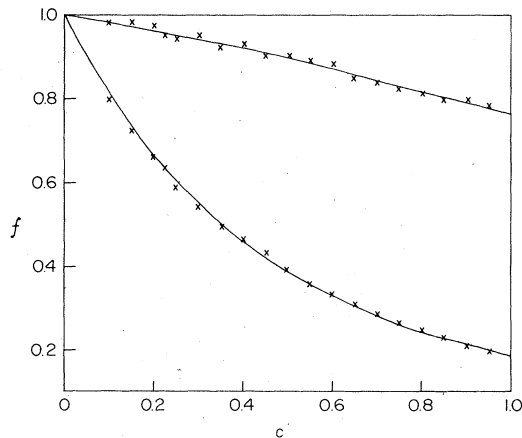


FIG. 2. Correlation factor $f(c)$ is plotted as a function of the concentration c for tracer diffusion in an anisotropic two-dimensional rectangular lattice for $J_x/J_y = \eta = 0.1$. The upper curve refers to $f_x(c)$, while the lower one gives $f_y(c)$. The crosses represent the simulation results obtained from samples with effective sizes of approximately 50 000 particles each.

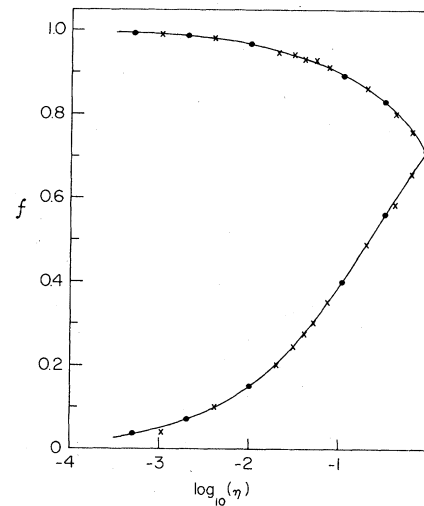


FIG. 3. Tracer diffusion correlation factors $f_x(c)$ (upper curve) and $f_y(c)$ (lower curve) are given as a function of $\log_{10}\eta$. The solid curves give our theoretical results, the solid circles are the precision simulation results using large samples, whereas the crosses refer to the less accurate simulation results obtained from small effective samples.

VI. CONCLUDING REMARKS

The resummation of the particle-vacancy composite pair scattering contributions, including the spatial constraints, leads to a good overall description of particle diffusion in both the isotropic and the anisotropic two-dimensional lattices. Another significant conclusion to be drawn from the good agreement between the simulations and the theory over more than three decades of the ratio η of the hopping rates along the two Cartesian axes is that the square root decrease in the diffusion coefficient along the fast direction, i.e.,

$$f_y(c) \rightarrow \text{const} \times \eta^{1/2}, \quad \eta \ll 1 \quad (6.1)$$

is an essentially correct universal feature of the problem. This square-root dependence was first predicted in Ref.

18. [Note that its form remains unaffected by the resummation described in the present work. Only the magnitude of the nonuniversal coefficient, labeled "const" in Eq. (6.1), is altered.]

Note added in proof. Recently, H. v. Beijeren and R. Kutner [Phys. Rev. Lett. 55, 238 (1985)] have independently observed the presence of the logarithmic terms [see our Eq. (3.1)]. Even their estimate for the correlation factor for the isotropic lattice at $c=0.5$ (see our Table I) is identical to ours, i.e., 0.7089 versus 0.710 ± 0.002 .

ACKNOWLEDGMENTS

This work was supported by the National Science Foundation under Grant No. DMR-83-12958. Helpful discussions with Professor K. Binder, Professor R. J. Elliott, Professor J. Gunton, Dr. K. Kehr, Dr. R. Stinchcombe, and Mr. P. Holdsworth are gratefully acknowledged.

¹For a recent review, see *Topics in Current Physics: Physics of Superionic Conductors*, edited by M. B. Salamon (Springer, Berlin, 1979).

²A comprehensive recent review and relevant bibliography is given by J. Völkl and G. Alefeld, in *Hydrogen in Metals: Topics in Applied Physics*, edited by G. Alefeld and J. Völkl (Springer, Berlin, 1978).

³See, for example, A. D. LeClaire, in *Physical Chemistry*, edited by H. Eyring, D. Henderson, and W. Jost (Academic, New York, 1970), Vol. 10.

⁴J. Bardeen and C. Herring, in *Imperfection in Nearly Perfect Crystals*, edited by W. Shockley (Wiley, New York, 1952), p. 261.

⁵J. R. Manning, *Diffusion Kinetics for Atoms in Solids* (Van Nostrand, New York, 1968).

⁶O. F. Sankey and P. A. Fedders, Phys. Rev. B 15, 3586 (1977); 20, 39 (1979); 22, 5135 (1980).

⁷P. A. Fedders and O. F. Sankey, Phys. Rev. B 15, 3580 (1977); 18, 5938 (1978).

⁸K. Nakazato and K. Kitahara, Prog. Theor. Phys. 64, 2261

(1980).

⁹R. A. Tahir-Kheli and R. J. Elliott, Phys. Rev. B 27, 844 (1983).

¹⁰G. E. Murch, Philos. Mag. 49, 21 (1984).

¹¹R. A. Tahir-Kheli, Phys. Rev. B 28, 3049 (1983).

¹²R. A. Tahir-Kheli, Philos. Mag. (to be published).

¹³For a recent review with many references to the earlier work, see G. E. Murch, in *Diffusion in Crystalline Solids*, edited by G. E. Murch and A. S. Nowick (Academic, New York, 1984), pp. 379–427.

¹⁴Another comprehensive review is by K. W. Kehr and K. Binder (unpublished); also see K. Kehr, R. Kutner, and K. Binder, Phys. Rev. B 23, 4931 (1981).

¹⁵H. J. De Bruin and G. E. Murch, Philos. Mag. 35, 1492 (1972).

¹⁶A. Sadiq and K. Binder, Surf. Sci. 128, 350 (1983).

¹⁷R. Kutner (unpublished).

¹⁸R. Tahir-Kheli, Phys. Rev. B 27, 6072 (1983).

¹⁹R. A. Tahir-Kheli, in *Essays in Theoretical Physics*, edited by W. E. Parry (Pergamon, New York, 1984).